

# Preparation of Molybdenum Carbides Using Butane and Their Catalytic Performance

Tian-cun Xiao,<sup>†</sup> Andrew P. E. York,<sup>†</sup> V. Cliff Williams,<sup>†</sup> Hamid Al-Megren,<sup>†</sup>  
Ahmad Hanif,<sup>†</sup> Xi-ya Zhou,<sup>‡</sup> and Malcolm L. H. Green<sup>\*,†</sup>

Wolfson Catalysis Centre, Inorganic Chemistry Laboratory, University of Oxford,  
South Parks Road, Oxford OX1 3QR, U.K., and Department of Materials,  
University of Oxford, Parks Road, Oxford OX1 3PH, U.K.

Received August 7, 2000. Revised Manuscript Received October 23, 2000

The synthesis of high surface area molybdenum carbides from molybdenum oxide and butane has been studied via temperature-programmed reaction (TPRe), X-ray diffraction (XRD), scanning electron microscopy (SEM), <sup>13</sup>C solid-state NMR, infrared (IR), and Raman spectroscopy (LR). The molybdenum oxygen/carbon system passes through four phase transitions before transforming into the pure Mo<sub>2</sub>C carbide. Carbon exists in two forms within high surface area molybdenum carbide. The initially produced molybdenum carbide has a face-centered-cubic (fcc) structure but is gradually converted into the hexagonal close-packed (hcp) structure with increasing carburization temperature, and eventually at high temperature coke is deposited. During the early stages, MoO<sub>3</sub> is reduced by H<sub>2</sub>, but at higher temperatures, butane also takes part in the reduction and, besides being consumed in the formation of carbide, is catalytically converted into methane, ethane, propane, and benzene. The high surface area of the molybdenum carbide materials is a consequence of preliminary cracking of oxide crystallites during reduction with hydrogen and later from the deposition of amorphous carbon. Catalytic activity tests indicate that molybdenum carbide material, prepared at 823 K, is a good catalyst for the dehydrogenation of butane. The carbide obtained between 923 and 973 K has excellent performance for pyridine HDN with good selectivity.

## Introduction

Early transition metal carbide of molybdenum and tungsten show catalytic properties similar to those of the noble metals<sup>1–4</sup> and so there is considerable interest in the possibility of using these refractory carbides and nitrides as novel catalysts as noble metal substitutes. In particular, the more recent development, of high surface area carbides, has led to an explosion of interest in their use. Consequently, carbides have been shown to be particularly active for hydrotreating, especially hydrodenitrogenation (HDN),<sup>5–16</sup> hydrogenation reac-

tions,<sup>17–24</sup> the Fischer–Tropsch reaction,<sup>20,23,24–28</sup> hydroisomerization,<sup>24,29–32</sup> and the oxyreforming of methane.<sup>33–35</sup>

The catalytic activity of molybdenum carbide materials is found to strongly related to their surface structure and elemental composition, which, in turn, depend on the method of synthesis. Some of the procedures developed for synthesizing high surface area molybdenum carbide materials include gas-phase reactions of volatile metal compounds,<sup>36–38</sup> reaction of gaseous reagents with solid-state metal compounds,<sup>39,40,41</sup> pyrolysis of metal

<sup>†</sup> Inorganic Chemistry Laboratory.

<sup>‡</sup> Department of Materials.

\* To whom correspondence should be addressed. Tel +44-1865-272649; Fax +44-1865-272690; e-mail malcolm.green@chem.ox.ac.uk.

(1) Gaziev, G. A.; Krylov, O. V.; Roginskii, S. Z.; Samsonov, G. V.; Fokina, E. A.; Yanovskii, M. I. *Dokl. Akad. Nauk S.S.S.R.* **1961**, *140*, 863.

(2) Muller, J.-M.; Gault, F. G. *Bull. Soc. Chim. Fr.* **1970**, *2*, 416.

(3) Sinfelt, J. H.; Yates, D. J. C. *Nature Phys. Sci.* **1971**, *229*, 27.

(4) Levy, R. B.; Boudart, M. *Science* **1973**, *181*, 547.

(5) Abe, H.; Cheung, T.-K.; Bell, A. T. *Catal. Lett.* **1993**, *21*, 11.

(6) Choi, J.-G.; Brenner, J. R.; Colling, C. W.; Demczyk, B. G.; Dunning, J. L.; Thompson, L. T. *Catal. Today* **1992**, *15*, 201.

(7) Colling, C. W.; Thompson, L. T. *J. Catal.* **1994**, *146*, 193.

(8) Lee, J. S.; Boudart, M. *Appl. Catal.* **1985**, *19*, 207.

(9) Markel, E. J.; Van Zee, J. W. *J. Catal.* **1990**, *126*, 643.

(10) Nagai, M.; Miyao, T. *Catal. Lett.* **1992**, *15*, 105.

(11) Nagai, M.; Miyao, T.; Tuboi, T. *Catal. Lett.* **1993**, *18*, 9.

(12) Schlatter, J. C.; Oyama, S. T.; Metcalfe, J. E.; Lambert, J. M., Jr. *Ind. Eng. Chem. Res.* **1988**, *27*, 1648.

(13) Abe, H.; Bell, A. T. *Catal. Lett.* **1993**, *18*, 1.

(14) Lee, K. S.; Abe, H.; Reimer, J. A.; Bell, A. T. *J. Catal.* **1993**, *139*, 34.

(15) Choi, J.-G.; Brenner, J. R.; Thompson, L. T. *J. Catal.* **1995**, *154*, 33.

(16) Yu, C. C.; Ramanathan, S.; Sherif, F.; Oyama, S. T. *J. Phys. Chem.* **1994**, *98*, 13038.

(17) Kojima, I.; Miyazaki, E.; Inoue, Y.; Yasumori, I. *J. Catal.* **1982**, *73*, 128.

(18) Leclercq, L.; Provost, M.; Pastor, H.; Leclercq, G. *J. Catal.* **1989**, *117*, 384.

(19) Lee, J. S.; Yeom, M. H.; Park, K. Y.; Nam, I.-S.; Chung, J. S.; Kim, Y. G.; Moon, S. H. *J. Catal.* **1991**, *128*, 126.

(20) Ranhotra, G. S.; Bell, A. T.; Reimer, J. A. *J. Catal.* **1987**, *108*, 40.

(21) Vidick, B.; Lemaitre, J.; Leclercq, L. *J. Catal.* **1986**, *99*, 439.

(22) Abe, H.; Bell, A. T. *J. Catal.* **1993**, *142*, 430.

(23) Djéga-Mariadassou, G.; Boudart, M.; Bugli, G.; Sayag, C. *Catal. Lett.* **1995**, *31*, 411.

(24) Sherif, F.; Vreugdenhil, W. *The Chemistry of Transition Metal Carbides and Nitrides*; Oyama, S. T., Ed.; Blackie Academic & Professional: Glasgow, 1996; pp 414–425.

(25) Park, K. Y.; Seo, W. K.; Lee, J. S. *Catal. Lett.* **1991**, *11*, 349.

(26) Liu, J.; Shen, J.; Gao, X.; Lin, L. *J. Therm. Anal.* **1993**, *40*, 1239.

(27) Dubois, J.-L.; Sayama, K.; Arakawa, H. *Chem. Lett.* **1992**, *5*.

(28) Leclercq, L.; Almazouari, A.; Dufour, M.; Leclercq, G. *The Chemistry of Transition Metal Carbides and Nitrides*; Oyama, S. T., Ed.; Blackie Academic & Professional: Glasgow, 1996; pp 345–361.

precursors,<sup>42</sup> and solution reactions.<sup>43,44</sup> Among these, one of the most promising and widely used is the gas-phase carburization of molybdenum oxides, developed by Boudart and co-workers.<sup>45–47</sup> However, there are many carbon sources for this carburization reaction, and it has become apparent that various carbon sources and conditions bestow different properties, structure, and catalytic performance on the resulting carbides.<sup>12,13,48–58</sup> To date, most of the work has focused on the use of mixtures of hydrogen and methane or ethane as carburizing agents. However, these gas mixtures are relatively unreactive and require the use of relatively high temperatures to affect carburization. The carbide products are limited to high-temperature phases only. There have been some reports of the use of higher alkanes as carbon sources, and generally those show greater reactivity as carburizing agents than CH<sub>4</sub> and C<sub>2</sub>H<sub>6</sub>. Therefore, we have studied the synthesis of molybdenum carbide materials using mixtures of hydrogen and butane for the carburization process, and the structure and catalytic performance of these carbides have been investigated, as described below.

## Experimental Section

The molybdenum carbides were prepared by temperature-programmed reduction of molybdenum trioxide (Alfa, 99.995%) at a rate of 1 K/min to different final temperatures. In all cases, 1.00 g of MoO<sub>3</sub> powder was loaded into the commercial Labcon silica microreactor (o.d. 10 mm) which has been described previously.<sup>59</sup> The carburizing atmosphere was composed of 5% C<sub>4</sub>H<sub>10</sub> (5 cm<sup>3</sup>/min, purity >99.99%) and 95% H<sub>2</sub> (95 cm<sup>3</sup>/min, purity >99.99%). This ratio was chosen on the basis of our earlier discovery that the most effective ratio for CH<sub>4</sub>/H<sub>2</sub> in the same carburization 20% CH<sub>4</sub> in H<sub>2</sub>. A total flowing rate of 100 cm<sup>3</sup>/min passed through the reactor, which was controlled by mass flow controllers (Brooks). When the temperature reached the maximum value, it was maintained for a further 2 h. Once the reaction was complete, the samples were quenched to room temperature under flowing argon by removing the tube from the furnace. Before exposure to the atmosphere, the samples were passivated in flowing 1 vol % O<sub>2</sub>/Ar (20 mL/min). The samples were carburized to final temperatures of 523, 673, 723, 823, 923, and 1023 K, and materials are denoted as MoC-523, MoC-673, MoC-723, MoC-823, MoC-923, and MoC-1023, respectively.

The changes of the MoO<sub>3</sub> during carburization were monitored by thermogravimetric analysis (TG, Rheometric Scientific STA 1500 equipped with a simultaneous thermal analyzer). A small quantity (approximately 30 mg) of MoO<sub>3</sub> was loaded into a small platinum crucible and placed into the balance in the instrument. The heating rate was controlled at 2 K/min, and a flowing atmosphere of 5% C<sub>4</sub>H<sub>10</sub> + 95% H<sub>2</sub> was maintained during carburization. An upper temperature limit of 1023 K was used, and to ensure complete reaction, the reaction was held at this temperature for a further 2 h.

The changes in the butane and product gases during the carburization were studied by TPRE methods. The reactor consisted of a 6 mm (o.d.) silica tube, into which 100 mg of MoO<sub>3</sub> was loaded and placed into a furnace. The temperature was increased at a rate of 2 K/min from room temperature to 1023 K and held for 1 h. The exit gas stream was passed through a filter and then into a GC-MS Hewlett-Packard 5890A gas chromatograph fitted with a Hewlett-Packard 5791A quadrupole mass spectrometer detector (MS). The masses 10–100 were scanned at 1 s intervals, which allowed the gases CO, CO<sub>2</sub>, H<sub>2</sub>O, CH<sub>4</sub>, C<sub>2</sub>H<sub>6</sub>, C<sub>6</sub>H<sub>6</sub>, C<sub>3</sub>H<sub>8</sub>, and C<sub>4</sub>H<sub>10</sub> to be monitored by their parent ions.

The crystalline components of the materials were identified by X-ray diffraction (XRD) using a Philips PW1710 diffractometer with Cu K $\alpha$  radiation. The morphology of the passivated samples was observed by scanning electron microscopy (SEM) on a Hitachi S-520 microscope operated at 20 kV and 40 mA. The powder sample was dispersed on the specimen stage with acetone.

Solid-state MAS NMR measurements were carried out in a CMX-200 NMR spectrometer at a frequency of 50.31 MHz. The strongly metallic samples were diluted to 40% with sodium chloride and ground finely before packing into the 7 mm zirconia rotor, fitted with boron nitride inserts. Typically 20 000 transients were collected using a single pulse (45°), with a pulse delay of 1.0 s and a 4 kHz spinning speed. The spectra were recorded at room temperature using adamantane ( $\delta = 29.5$ ) as the reference.

Infrared (IR) spectra of the carburized samples were recorded with a Perkin-Elmer Paragon 1000 FT-IR as KBr pellets containing ca. 1–2 wt % of sample powder, using 16 scans at 4 cm<sup>-1</sup> resolution. Raman spectra were recorded in air with a resolution of 2 cm<sup>-1</sup> using a Yvon Jobin Labram spectrometer, using a 632 nm HeNe laser, run in a backscat-

(29) Pham-Huu, C.; York, A. P. E.; Benaissa, M.; Del Gallo, P.; Ledoux, M. J. *Ind. Eng. Chem. Res.* **1995**, *34*, 1107.

(30) Keller, V.; Weher, P.; Garin, F.; Ducros, R.; Maire, G. *J. Catal.* **1995**, *153*, 9.

(31) Lee, J. S.; Song, B. J.; Li, S.; Woo, H. C. *The Chemistry of Transition Metal Carbides and Nitrides*; Oyama, S. T., Ed.; Blackie Academic & Professional: Glasgow, 1996; pp 398–413.

(32) Ledoux, M. J.; Pham-Huu, C.; York, A. P. E.; Blekkan, E. A.; Delporte, P.; Del Gallo, P. *The Chemistry of Transition Metal Carbides and Nitrides*; Oyama, S. T., Ed.; Blackie Academic & Professional: Glasgow, 1996; pp 373–397.

(33) York, A. P. E.; Claridge, J. B.; Brungs, A. J.; Tsang, S. C.; Green, M. L. H. *Chem. Commun.* **1997**, 39.

(34) York, A. P. E.; Claridge, J. B.; Márquez-Alvarez, C.; Brungs, A. J.; Tsang, S. C.; Green, M. L. H. *Stud. Surf. Sci. Catal.* **1997**, *110*, 711.

(35) Claridge, J. B.; York, A. P. E.; Brungs, A. J.; Márquez-Alvarez, C.; Sloan, J.; Tsang, S. C.; Green, M. L. H. *J. Catal.* **1998**, *180*, 85.

(36) O'Brien, R. J.; Xu, L.; Bi, X. X.; Eklund, P. C.; Davis, B. H. *The Chemistry of Transition Metal Carbides and Nitrides*; Oyama, S. T., Ed.; Blackie Academic & Professional: Glasgow, 1996; pp 362–372.

(37) Ledoux, M. J.; Pham-Huu, C. *Catal. Today* **1992**, *15*, 263.

(38) Ledoux, M. J.; Hantzer, S.; Pham-Huu, C.; Guille, J.; Desaneux, M.-P. *J. Catal.* **1988**, *114*, 176.

(39) Oyama, S. T. *The Chemistry of Transition Metal Carbides and Nitrides*; Oyama, S. T., Ed.; Blackie Academic & Professional: Glasgow, 1996; pp 1–27.

(40) Chorley, R. W.; Lednor, P. W. *Adv. Mater.* **1991**, *3*, 474.

(41) Leclercq, L.; Provost, M.; Pastor, H.; Grimblot, J.; Hardy, A. M.; Gengembre, L.; Leclercq, G. *J. Catal.* **1989**, *117*, 371.

(42) Giraudon, J.-M.; Leclercq, L.; Leclercq, G.; Lofberg, A.; Frennet, A. *J. Mater. Sci.* **1993**, *28*, 2449.

(43) Zeng, D.; Hampden-Smith, M. J. *Chem. Mater.* **1993**, *5*, 681.

(44) Zeng, D.; Hampden-Smith, M. J. *Chem. Mater.* **1992**, *4*, 968.

(45) Volpe, L.; Boudart, M. *J. Solid State Chem.* **1985**, *59*, 348.

(46) Volpe, L.; Boudart, M. *J. Solid State Chem.* **1985**, *59*, 332.

(47) Wroblewski, J. T.; Boudart, M. *Catal. Today* **1992**, *15*, 349.

(48) Chen, J. G. *J. Catal.* **1995**, *154*, 80.

(49) Chen, J. C.; Fruhberger, B.; Weisel, M. D.; Baumgartner, J. E.; De Vries, B. D. *The Chemistry of Transition Metal Carbides and Nitrides*; Oyama, S. T., Ed.; Blackie Academic & Professional: Glasgow, 1996; pp 439–454.

(50) Choi, J. G.; Jung, M. K.; Choi, S.; Park, T. K.; Kuk, I. H.; Yoo, J. H.; Park, H. S.; Lee, H. S.; Ahn, D. H.; Chung, H. S. *Bull. Chem. Soc. Jpn.* **1997**, *70*, 993.

(51) Meunier, F.; Delporte, P.; Heinrich, B.; Bouchy, C.; Crouzet, C.; Pham-Huu, C.; Panissod, P.; Lerou, J. J.; Mills, P. L.; Ledoux, M. J. *J. Catal.* **1997**, *169*, 33.

(52) Schwartz, V.; Oyama, S. T. *Chem. Mater.* **1997**, *9*, 3052.

(53) Choi, J. G.; Oh, H. G.; Baek, Y. S. *J. Ind. Eng. Chem. Res.* **1965**, *4*, 94.

(54) Kim, H. S.; Bugli, G.; Djéga-Mariadassou, G. *J. Solid State Chem.* **1999**, *142*, 100.

(55) Decker, S.; Lofberg, A.; Bastin, J. M.; Frennet, A. *Catal. Lett.* **1997**, *44*, 229.

(56) Li, S. Z.; Kim, W. B.; Lee, J. S. *Chem. Mater.* **1998**, *10*, 1853.

(57) Gallo, P. D.; Meunier, F.; Pham-Huu, C.; Crouzet, C.; Ledoux, M. J. *Ind. Eng. Chem. Res.* **1997**, *36*, 4166.

(58) Claridge, J.; York, A. P.; Brungs, A. J.; Green, M. L. H. *Chem. Mater.*, in press.

(59) Claridge, J. B.; Green, M. L. H.; Tsang, S. C.; York, A. P. E. *Appl. Catal.* **1992**, *89*, 103.

tered confocal arrangement. The sample was pressed into a self-supporting pellet for the average measurement.

Catalyst surface areas were determined from N<sub>2</sub> BET isotherms. The carbon content of the samples was measured by the Micro-analytical Department at Inorganic Chemistry Oxford.

For the study of pyridine HDN over the molybdenum carbides, the activity was accessed using a 6.0 mm (o.d.) silica reactor. Approximately 0.2 g of catalyst was loaded onto a plug of silica wool, and the temperature of the catalyst bed was measured with a thermocouple inserted directly into the bed. The catalyst was heated under H<sub>2</sub> from room temperature to 773 K at a rate of 2 K/min, held at 773 K for 1 h, and then cooled to 653 K before pyridine was introduced for the reaction. The reactants passed over the catalyst (total pressure ~101 kPa) consisting of flowing H<sub>2</sub> at a rate of 20 mL/min saturated with pyridine (99.9%, Aldrich) at 273 K (0.61 kPa). The products were analyzed using a Hayesep D packed column and analyzed using a HP 5890 GC equipped with a TCD and FID.

Catalytic reactions for the dehydrogenation of *n*-butane over the carbide catalyst were carried out in a fixed-bed continuous-flow 6 mm (o.d.) silica microreactor. The catalyst powder (0.1 g) was loaded into the reactor and first purged with H<sub>2</sub> at 823 K for 2 h followed by the introduction of *n*-butane at a space velocity of 1000 h<sup>-1</sup>. The products were analyzed by an on-line 5890 GC in with a 2 m long Porapak Q column and detected by both TCD and FID.

## Results

**Structure Changes of the Carbides during Carburization at Different Temperatures.** A series of molybdenum carbides were synthesized under an atmosphere of 5% C<sub>4</sub>H<sub>10</sub> and 95% H<sub>2</sub>, using temperature-programmed reduction to different final carburization temperatures, which were held at the final temperature for a further 2 h. Figure 1 shows the XRD patterns of the prepared samples; pattern a corresponds to the starting MoO<sub>3</sub> phase. Upon reduction of the MoO<sub>3</sub> with 5% C<sub>4</sub>H<sub>10</sub> + 95% H<sub>2</sub> at 523, 623, 673, and 723 K, the diffraction peaks at 26.03°, 37.02°, and 53.5° are displayed in all cases, which are the typical patterns of monoclinic MoO<sub>2</sub>.<sup>60</sup> When the reduction temperature was raised to 823 K, the diffraction patterns became very weak, and only two very broad peaks at 37° and 63° appeared. These are attributed to the diffraction pattern caused by a fcc arrangement of molybdenum atoms, presumably MoC<sub>1-x</sub><sup>61</sup> or molybdenum oxycarbide,<sup>32</sup> because, as shown later, there is still some oxygen present in this sample. However, the oxycarbide has a similar XRD diffraction pattern to that of MoC<sub>1-x</sub>. Carburization at temperatures up to 923 K for 2 h allows retention of this structure; however, diffraction peaks at 34.3°, 37.9°, 39.5°, and 52.2° appeared in the sample carburized to 1023 K, corresponding to the diffraction peaks of [100], [002], [101], and [102] planes of hexagonal Mo<sub>2</sub>C (*P63/mmc*).<sup>62</sup> Thus, carburization at 1023 K changes the faced-centered-cubic lattice to hexagonal-close-packed Mo<sub>2</sub>C.

The change of carbon and hydrogen content with the carburization temperature is shown in Figure 2. For the samples carburized at temperatures lower than 523 K, the carbon content was very low, almost undetectable. Carburization with butane from 723 to 823 K increased the carbon content in the samples quickly, to a maxi-

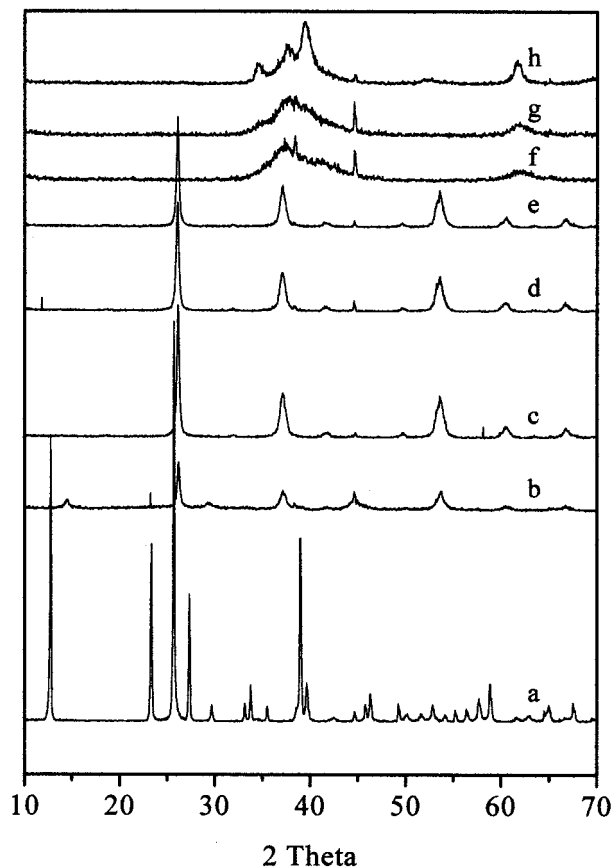


**Figure 1.** XRD of the molybdenum carbides synthesized with butane at different temperatures.

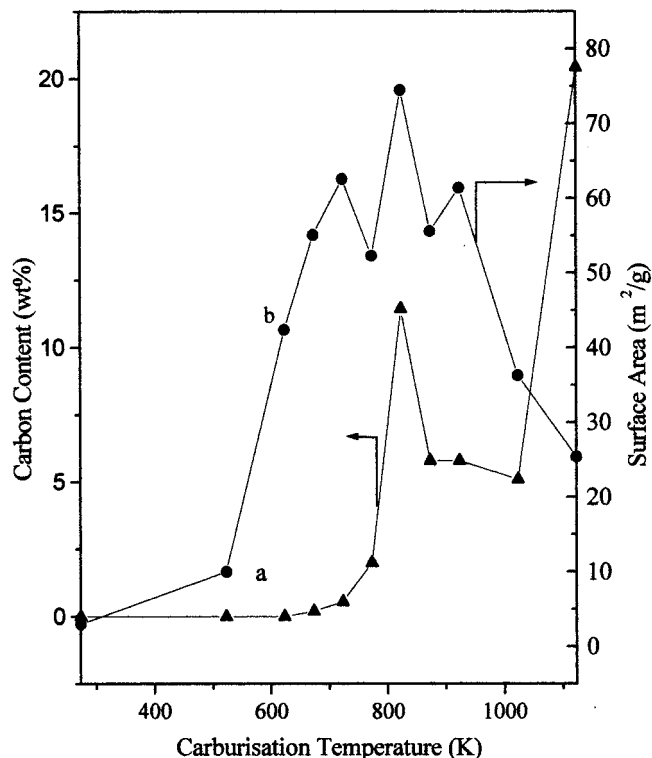


**Figure 2.** Changes of carbon content and surface area in molybdenum trioxide carburized with butane and hydrogen at different temperatures.

(60) . Natl. Bur. Stand. (US), Monogr. **1981**, 25, 18–44.

(61) Lander, Germer Trans. Am. Inst. Min. Eng. **1948**, 175, 648.

(62) Tutiya, H. Bull. Inst. Chem. Res. Kyoto Univ. **1932**, 11, 1150.

um of 12% corresponding to a value expected for bulk carbide formation MoC<sub>(1-x)</sub> or insertion of much carbon

atom in the lattice of molybdenum oxide to form molybdenum oxycarbide. Beyond this temperature, the carbon content decreased and remained at approximately 5.5% for the temperature range 873–1023 K and then increased sharply when the carburization reaction was performed at 1123 K; this was due to the occurrence of carbon deposition.

BET surface area measurements showed that the surface area of the starting  $\text{MoO}_3$  sample is less than  $3.0 \text{ m}^2/\text{g}$ . The surface areas of the samples increased rapidly when carburized in the temperature range 523–723 K, which indicates that the surface area increases during the reduction of  $\text{MoO}_3$  to  $\text{MoO}_2$ . However, at 773 K, the surface area of the carburized sample decreased slightly to  $55 \text{ m}^2/\text{g}$ . This may be the result of sintering of the  $\text{MoO}_2$  oxide, especially considering the relatively low carbon content achieved at this temperature. The sample carburized at 823 K has the highest surface area, at  $75 \text{ m}^2/\text{g}$  at this temperature, at which the XRD data show the monoclinic  $\text{MoO}_2$  is converted to fcc molybdenum carbide phase. The surface area of the carbide prepared at 873 K decreased with increasing temperature to  $37 \text{ m}^2/\text{g}$  for the MoC-1023 sample, presumably as a result of sintering. Above the carburization temperature of 1023 K, the surface area decreases further; however, this sample was composed of both the carbide and bulk carbon.

Figure 3 shows the Raman spectra of  $\text{Mo}_2\text{C}$  carburized at different temperatures. The initial oxide shows at 995, 819, 701, 666, 417, 377, 338, 291, and  $217 \text{ cm}^{-1}$ . The Raman at  $819 \text{ cm}^{-1}$  is the most intense. The bands at 995 and  $377 \text{ cm}^{-1}$  can be attributed to the symmetric stretching and bending modes of the O–Mo–O bonds of octahedrally coordinated polymeric molybdenum oxide.<sup>63–65</sup> After temperature-programmed treatment with  $\text{H}_2$  and  $\text{C}_4\text{H}_{10}$  up to 523 K, almost no changes were observed in the Raman bands of the materials. After reduction at 623 K for 2 h, the bands at 701, 417, and  $219 \text{ cm}^{-1}$  had disappeared, and the other bands were broadened. When the reduction temperature was increased, all of the Raman bands weakened, and at 773 K, there was virtually no spectrum. These changes are consistent with the strong absorption of the excitation source. The samples are now black, and this suggests there will be metallic conductivity at the surface. Further, the XRD pattern of the sample indicates the presence of the  $\text{MoO}_2$  phase, as does the carbon content data (although by 773 K, the 2% carbon content indicates that carbide formation has started). It appears that surface carbide formation starts at temperatures above 673 K, and thus is some 100 K lower than is required to carburize the bulk sample.

Figure 4 shows the IR spectra of molybdenum oxycarbide materials carburized at different temperatures. After treatment at 523 K, the IR spectrum is identical to that of  $\text{MoO}_3$ . Raising the reaction temperature to 623 K gives new bands, characteristic of  $\text{MoO}_2$ . Further carburization gives black metallic materials with no IR features.

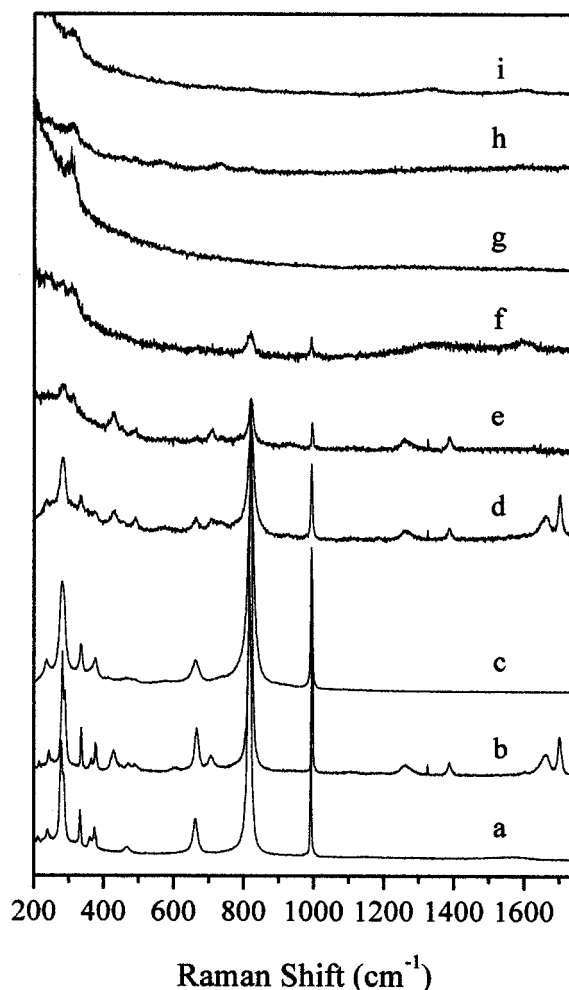


**Figure 3.** Laser Raman spectra of the molybdenum trioxide carburized with butane and hydrogen at different temperatures.

The morphology of materials after reactions of  $\text{MoO}_3$  at different temperatures has been observed by SEM; the data are shown in Figure 5. Commercial molybdenum trioxide crystals are platelets with lengths up to  $10 \mu\text{m}$ . After reaction at 523 K for 3 h, the morphology of the particles was unchanged. Upon raising the carburization temperature to 623 K, the morphology of the sample became irregular, and many star cracks appeared on the surface of the platelets (Figure 5c). This is consistent with the phase change and lattice contraction produced upon reduction of  $\text{MoO}_3$  to  $\text{MoO}_2$ . After treatment with butane and hydrogen at 723 K, the molybdenum sample showed more cracks on the surface of the platelets, and some of the particles appeared to have shattered to give crystallites that are several micrometers wide and up to  $5 \mu\text{m}$  in length. After the sample was carburized at 823 K for 3 h, some of the material appeared as sticklike particles, but still a considerable proportion of crystallites remain which had retained their parent  $\text{MoO}_3$  morphology. After reaction at 923 K for 3 h, there was little further change. The morphology of the sample after further carburization at 1023 K for 3 h had changed to rectangular particles, less than  $10 \mu\text{m}$  in dimensions. This is attributed to sintering (in agreement with the BET surface area measurements). The surface of the cracked materials (MoC-823) from examining a magnification of 2K is

(63) Kasztelan, S.; Grimbolot, J.; Bonnelle, J. P.; Payen, E.; Touhoat, H.; Jacquin, Y. *Appl. Catal.* **1983**, *7*, 191.

(64) Kasztelan, S.; Payen, E.; Touhoat, H.; Grimbolot, J.; Bonnelle, J. P. *Polyhedron* **1986**, *5*, 157.

(65) Ng, K. Y. S.; Gulari, E. *J. Phys. Chem.* **1985**, *89*, 2479.

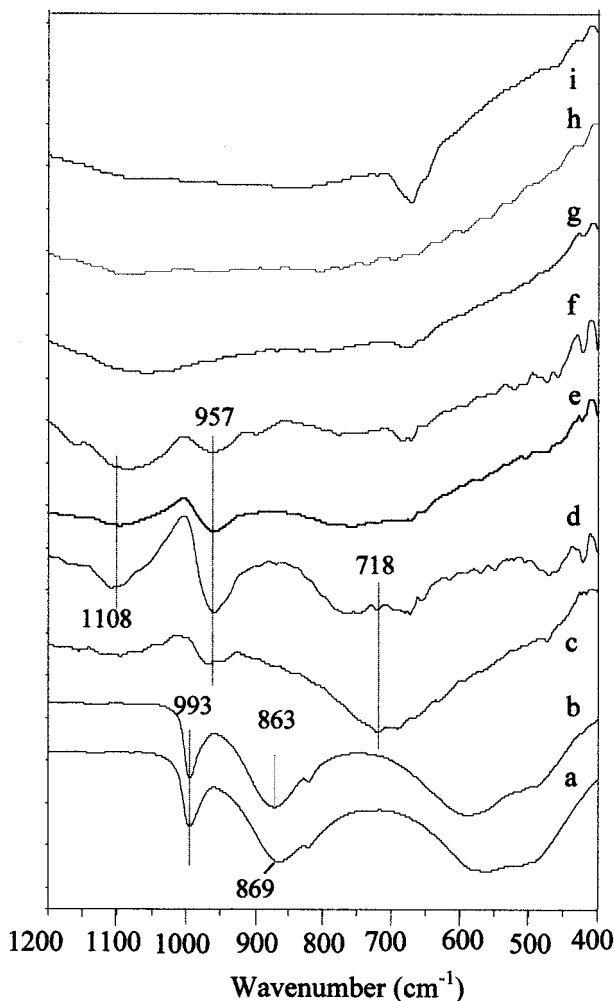


**Figure 4.** IR spectra of the molybdenum trioxide carburized with butane and hydrogen at different temperatures.

shown in Figure 5h. Besides the larger star cracks, there are also many small holes present on the highly pitted surface. These voids must be partly responsible for the high surface area of the resulting carbide.

The  $^{13}\text{C}$  MAS NMR data for the carburized materials prepared at different temperatures are shown in Figure 6. At 623 K, the material showed only one broad peak at 113 ppm. This peak is assigned by comparison with a sample that was prepared using the published procedure,<sup>66</sup> carbon located within a fcc molybdenum lattice. The Raman spectra show there is no bulk carbon deposition in these samples; hence, the NMR signals are assigned to the carbon located in the carbide lattice. This peak became more intense in material from higher temperature carburization. For the materials formed after reaction at 823 K, two new peaks showed at 273 ppm which was assigned by comparison to hcp  $\text{Mo}_2\text{C}$  (Aldrich) and a less intense peak at 208 ppm, which is a spinning sideband. The substantial difference existing between the chemical shift of carbon in fcc and hcp molybdenum carbide is surprising. It may be due to the different structure or possibly the presence of oxygen in the fcc molybdenum carbide. The materials prepared at 1023 K showed peaks at 273 and 113 ppm, both

become sharper, suggesting sintering had occurred. Thus, NMR data are consistent with the transformation of fcc molybdenum carbide or oxycarbide to the hcp  $\text{Mo}_2\text{C}$  phase. It is interesting to note the persistence of the fcc-based carbide phase over the 400 K temperature range. This is not suggested by XRD, which shows only the arrangement of the phase with the greatest long-range order, and thus for the most part, the molybdenum carbide or oxycarbide with fcc structure is not detected.

There are few reports of the solid-state NMR.<sup>67,68</sup> The  $^{13}\text{C}$  NMR chemical shift of hexagonal molybdenum carbide has been reported at 273 ppm<sup>67</sup> in agreement with our data. The  $^{13}\text{C}$  NMR peak at 113 ppm has been observed before<sup>69</sup> and was assigned to amorphous carbon deposited on the catalyst. However, bulk carbon deposition is not expected to occur until temperatures reach 900 K. Also, as noted, a large amount of oxygen held within the material up to 950 K. This implies that the phases produced up until this temperature are best represented as  $\text{MoC}_x\text{O}_y$  rather than being the pure binary carbides. Therefore, we assign the peak at 113 ppm to carbon atom within  $\text{MoO}_x\text{C}_y$  with fcc structure.

**Monitoring the Carburization of  $\text{MoO}_3$  with a Mixture of Hydrogen and Butane.** TG-DTA analysis was carried out at  $\text{MoO}_3$  (30 mg) treated with a heating rate of  $2\text{ K min}^{-1}$  in a flow of  $50\text{ cm}^3\text{ min}^{-1}$  of a mixture of butane in hydrogen. The final temperature of 973 K was held for 2 h in line with the experiments of TPREMS and carbide preparation. The data are shown in Figure 7. Four stages of weight loss were observed during the carburization of the  $\text{MoO}_3$ . The first stage occurred in the range 473–693 K, and the sample weight decreased very slowly by about 0.35 mg. From 693 to 910 K, a 4.0 mg weight loss occurred, which is a greater weight loss than expected for simply reduction of  $\text{MoO}_3$  to  $\text{MoO}_2$  (2.9 mg). The sharp weight loss in the temperature range 920–950 K was 3.0 mg; the minimum weight at 21.5 mg corresponds to a little above that expected for pure  $\text{Mo}_2\text{C}$ . The weight of the sample increased continuously from 21.5 to 25.0 mg from 950 to 973 K but remained the same hereafter. The final increase of the sample weight is caused by carbon deposition on the active surface.

From the DTA curves, it can be seen that reaction of  $\text{MoO}_3$  with a mixture of  $\text{H}_2$  and butane is endothermic from room temperature to 820 K. From 820 to 960 K, a large exothermic change occurred which is probably due to the phase change from fcc  $\text{MoC}_{(1-x)}$  to  $\text{Mo}_2\text{C}$ .

Figure 8 shows the distribution of volatile products during carburization of  $\text{MoO}_3$  with 95%  $\text{H}_2$  + 5%  $\text{C}_4\text{H}_{10}$ . The profiles of  $m/e = 16, 18, 28, 30, 44,$  and  $78$  correspond to methane, water, carbon monoxide, ethane, carbon dioxide, and benzene, respectively. The peaks at 39, 43, and 44 can all be attributed to fragments derived from butane. The reaction was monitored from room temperature to 690 K; only the signals associated with

(67) Ledoux, M. J.; Pham-Huu, C.; Delporte, P.; Blekkan, E. A.; York, A. P. E.; Derouane, E. G.; Fonseca, A. *Stud. Surf. Sci. Catal.* **1995**, *92*, 81.

(68) Meunier, F.; Delporte, P.; Heinrich, B.; Bouchy, C.; Crouzet, C.; Pham-Huu, C.; Panissod, P.; Lerou, J.; Mills, P. L.; Ledoux, M. J. *J. Catal.* **1997**, *169*, 33.

(69) Kellberg, L.; Zeuthen, P.; Jakobsen, H. J. *J. Catal.* **1993**, *143*, 45.

(66) Lee, J. S.; Volpe, L.; Ribeiro, F. H.; Boudard, M. *J. Catal.* **1988**, *112*, 44.

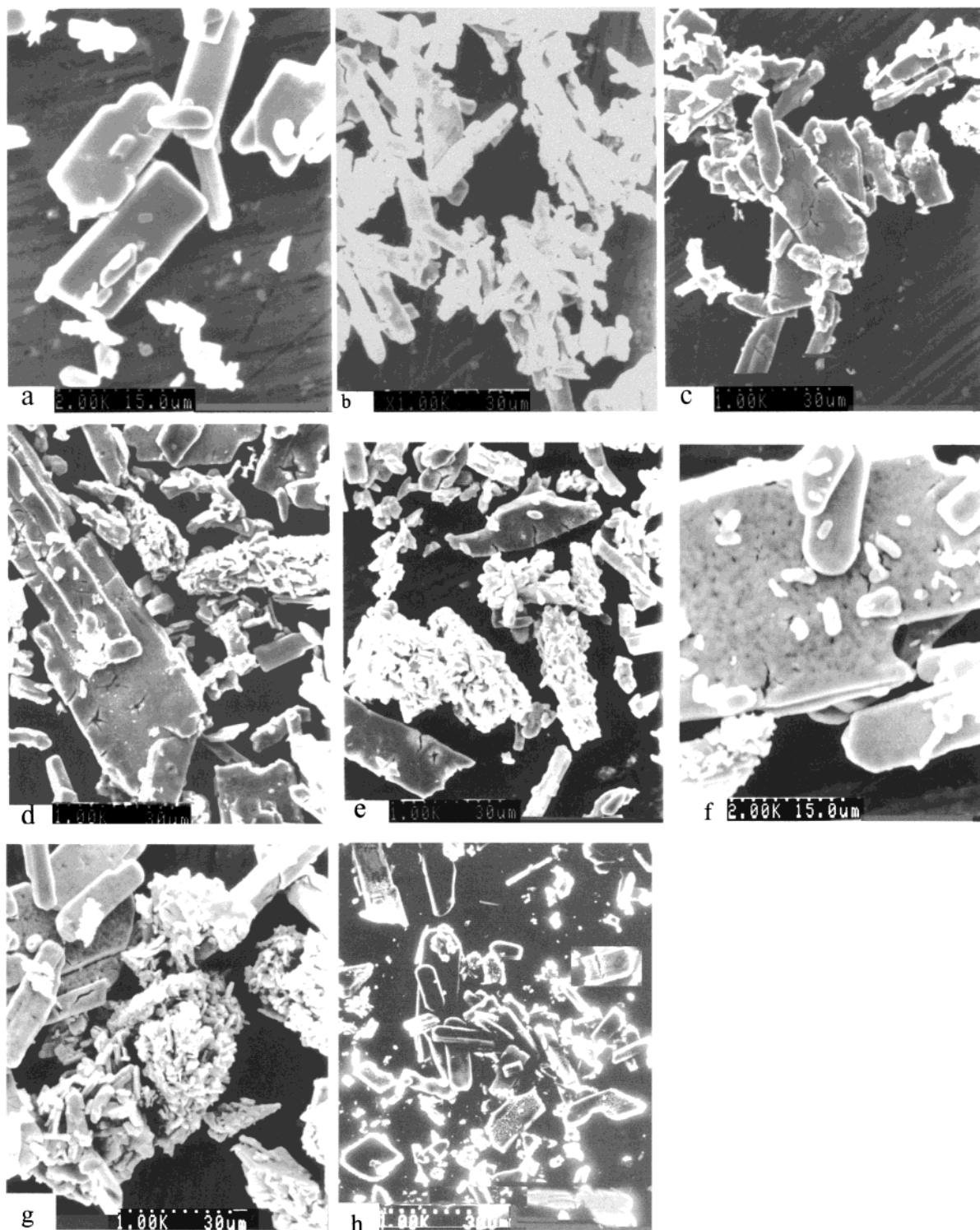


**Figure 5.** SEM graphs of MoO<sub>3</sub> carburized with butane and hydrogen at different temperatures.

butane were observed. When the temperature reached 720 K, water was observed, but there were no changes in signals associated with butane, implying that the water was formed by the reduction of MoO<sub>3</sub> with hydrogen and that butane was not involved in the reduction of this stage. Further increase of the temperature caused the peaks associated with butane to decrease and reached a minimum at 793 K. Meanwhile, the signals of  $m/e = 18$  and 44 due to H<sub>2</sub>O and CO<sub>2</sub> appeared. This contrasts with the reduction of MoO<sub>3</sub> with methane or ethane, in which no CO<sub>2</sub> was produced up to 793 K,<sup>70</sup> so that butane is more active than

methane or ethane for preparing carbides at lower temperatures. The signals due to methane, ethane, propane, and benzene start to appear at 793 K, suggesting the butane is undergoing hydrocracking and dehydrogenation to benzene on the partially reduced and carburized MoO<sub>3</sub>. The maximum production of benzene ( $m/e = 78$ ) occurred at 872 K, which correlates closely with the peak associated with ethane. At 890 K, a maximum in CO production was observed, and by 898

(70) Decker, S.; Lofberg, A.; Bastin, J. M.; Frennet, A. *Catal. Lett.* **1997**, *44*, 229.

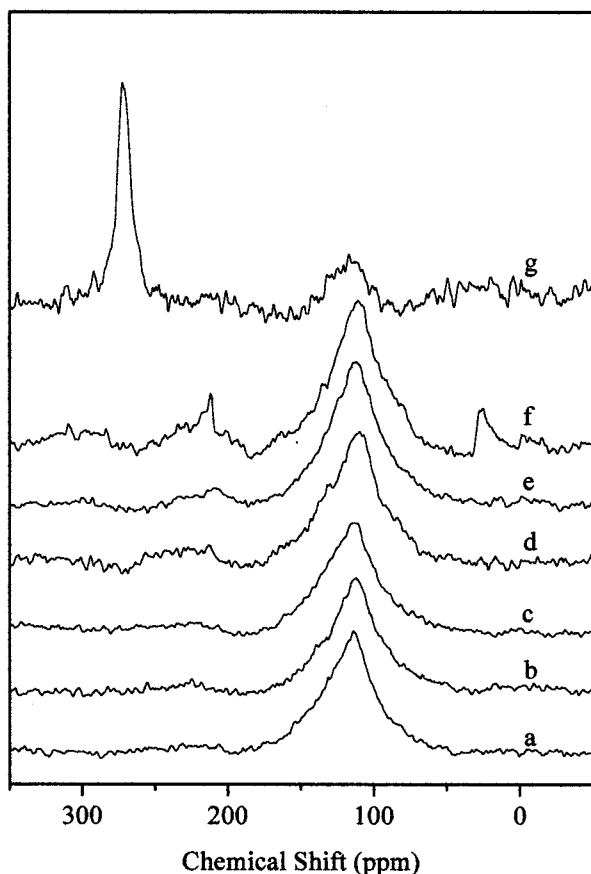


**Figure 6.**  $^{13}\text{C}$  MAS NMR spectra of  $\text{MoO}_3$  carburized with hydrogen and butane at different temperatures.

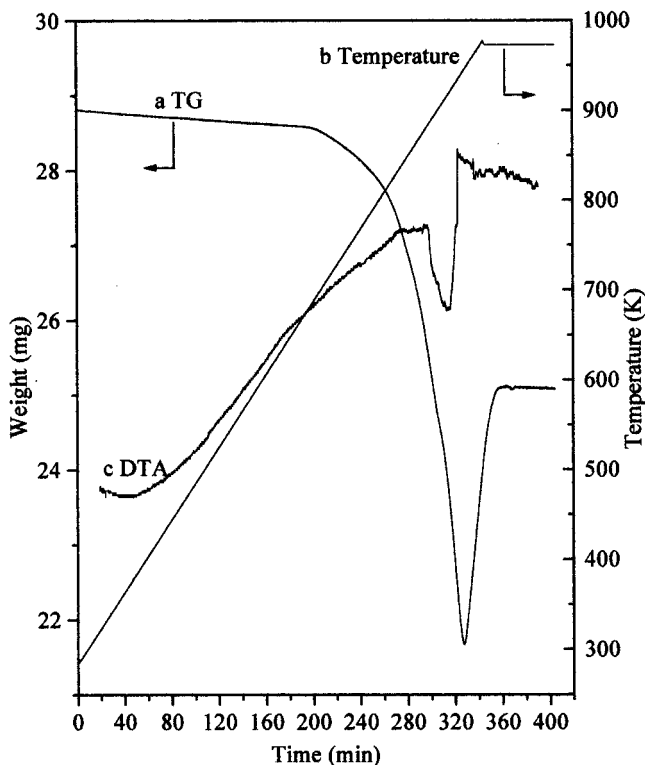


**Figure 7.** TG-DTA curves of  $\text{MoO}_3$  under the atmosphere of  $\text{H}_2 + \text{C}_4\text{H}_{10}$ .

K, the peaks for water, methane, carbon monoxide, and carbon dioxide had appeared, coupled with a sharp decrease of the identity of peaks associated with butane.

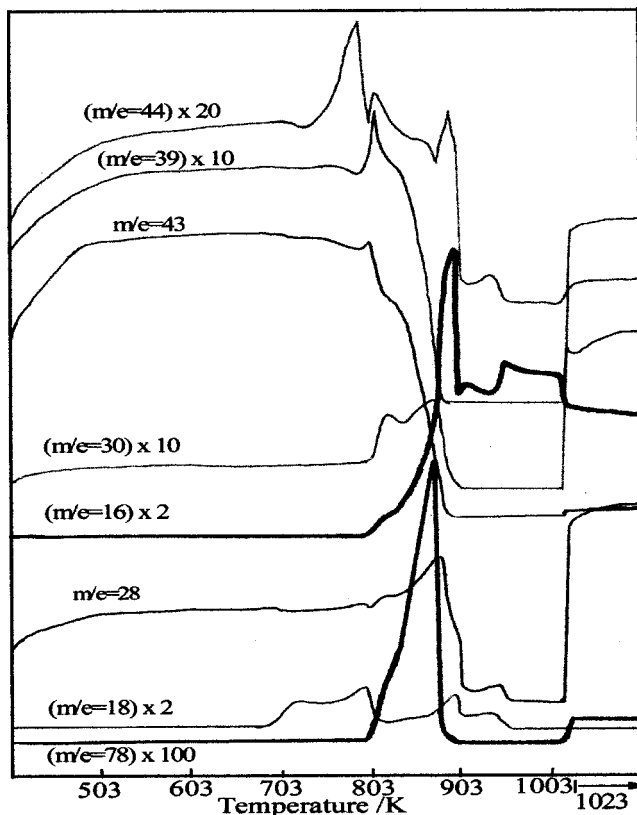


**Figure 8.** TPRE-MS of  $\text{MoO}_3$  during carburization of  $\text{MoO}_3$  with butane and hydrogen.

Thus, butane is converted into methane, carbon monoxide, carbon dioxide, and also probably to deposited carbon. Above 897 K, butane is completely converted to methane and thus continues the carburization process. When the temperature reaches 950 K, the fourth maximum of water production appeared accompanied by the peaks of CO and  $\text{CO}_2$  and a decrease in methane formation. This shows the last remnants of molybdenum oxide are reduced. Above 950–1013 K, the signals due to carbon products were all relatively weak, showing that carbon deposition was occurring. Above 1023 K, the main reaction products were methane, ethane, and propane. According to our XRD results, the molybdenum carbide was fully formed when the reduction temperature was 823 K. However, the TPRE-MS data show there are still some oxygen-containing compounds like water and carbon oxides formed in a further reduction with  $\text{C}_4\text{H}_{10}$  and  $\text{H}_2$ . Therefore, it seems that the molybdenum carbide synthesized at temperatures lower than 950 K still contains oxygen in the fcc carbide lattice as molybdenum oxycarbide materials, as suggested by Oyama<sup>71</sup> and Ledoux.<sup>32</sup>

#### Catalytic Activity of Molybdenum Carbide for Pyridine HDN and Dehydrogenation of Butane.

The catalytic activities of samples of molybdenum carbide prepared at 823, 873, and 1023 K have been tested for pyridine HDN using 1 atm of hydrogen. As shown in Figure 9, the conversion of pyridine using MoC-873 K was nearly 100%, but for MoC-823 K, it was only 45% at first. The MoC-1023 K catalyst had the lowest activity. Unfortunately, the activities of all the three catalysts decreased with time, and MoC-823 K

(71) Oyama, S. T.; Yu, C.; Ramanathan, S. *J. Catal.* **1999**, *184*, 535.

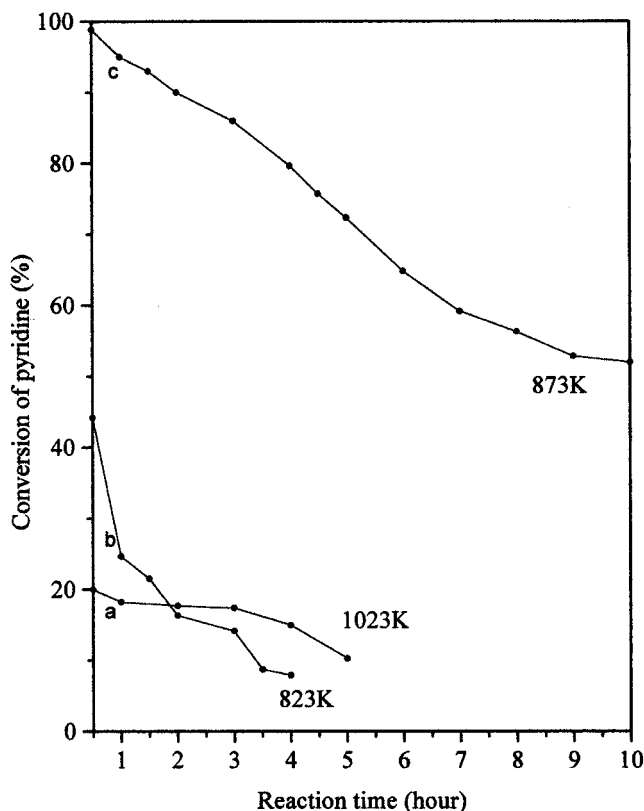


**Figure 9.** Pyridine HDN activity over molybdenum carbides prepared with butane and hydrogen at different temperatures.

activity decreased the fastest. After 4 h on stream, the activity of MoC-823 K was about 10%, and that of MoC-1023 K was less than 20%. All three carbide catalysts are not stable; hence, the preliminary pyridine HDN rate is calculated on the basis of preliminary conversion of pyridine at 650 K and 101 kPa. The pyridine conversion rate is 0.51 nmol/(g s) over MoC-873 K, 0.22 nmol/(g s) over MoC-823 K, and 0.09 nmol/(g s) over MoC-1023 K. MoC-873 K is not only more active than the other two catalysts but also more stable. Pyridine conversion over it was still nearly 70% after 5 h reaction.

The MoC-873 K catalyst was more active for pyridine HDN than molybdenum carbide prepared using methane.<sup>72,73</sup> The lower activity of MoC-1023 K possibly resulted from its hexagonal structure, which may not be as active as the molybdenum carbide with fcc structure (hcp molybdenum carbide is prepared from methane) although this catalyst also has a considerably lower surface area than either of the other two systems. The main products of the HDN reaction were butane, pentane, and cyclopentane, showing that molybdenum carbide prepared using butane has good selectivity.

As shown from the TPRE-MS results, during carburization of MoO<sub>3</sub>, some benzene was produced in the temperature range 793–897 K even though the hydrogen concentration was 20 times higher than the butane, suggesting that fcc molybdenum carbide materials, which also contains a high oxygen content, is active for

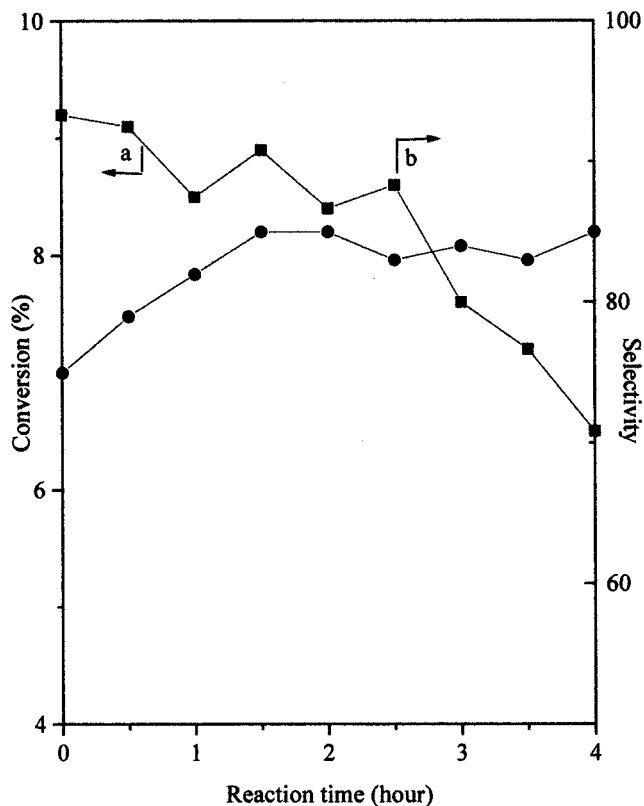


**Figure 10.** Activity of dehydrogenation of *n*-butane over molybdenum carbide prepared with butane at 823 K.

dehydrogenation of butane under carefully controlled conditions. Moreover, conversion of low-cost liquefied petroleum gas (LPG) into valuable aromatics is a very important reaction.<sup>74</sup> Therefore, we prepared molybdenum carbides by temperature-programmed carburization with 5% C<sub>4</sub>H<sub>10</sub> + 95% H<sub>2</sub> at a rate of 2 K/min to 823 K and held the catalyst at 823 K for a further 30 min, before changing the gas feed to pure C<sub>4</sub>H<sub>10</sub> at a GHSV of 1000 h<sup>-1</sup>. The conversion of butane was around 9% during the first 30 min, and the product was mainly benzene. But after 4 h on stream, the conversion had slowly decreased to 6.4% (Figure 10). This activity was higher than that obtained for the commercial Ga/ZSM-5 catalyst.<sup>75</sup> The selectivity to benzene remained constant at around 80%, which suggests that fcc MoO<sub>x</sub>C<sub>y</sub> or MoC<sub>(1-x)</sub> is also quite active and selective for the dehydrogenation of butane to benzene. Further studies will be made on the optimization of molybdenum carbide preparation for this reaction.

## Discussion

**Phase Transformation of MoO<sub>3</sub> during Carburization with Butane.** There have been several studies<sup>56,58,68</sup> on the phase transitions occurring during carburization of MoO<sub>3</sub> with methane and ethane. The reaction of MoO<sub>3</sub> with ethane proceeds topotactically, while with methane it does not. It has been proposed that the intermediate phases between MoO<sub>3</sub> and Mo<sub>2</sub>C include MoO<sub>2</sub> and MoO<sub>x</sub>C<sub>y</sub><sup>56,57</sup> and that formation of

(72) Choi, J. G.; Brenner, J. R.; Thompson, L. T. *J. Catal.* **1995**, *154*, 33.

(73) Xiao T.-C.; Al-Megren, H.; York, A. P. E.; Claridge, J. B.; Wang, H.-T.; Sloan, J.; Green, M. L. H. *12<sup>th</sup> Jaques Cartier Meeting, Clean Processes and Environment: The Catalytic Solution*, Poster 17, Lyon France, Dec 6, 1999.

(74) Doolan, P. C.; Pujado, P. R. *Hydroc. Process.* Sept **1989**, *68*, 72.

(75) Mao, R. L. V.; Carli, R.; Yao J. H.; Ragaini, V. *Catal. Lett.* **1992**, *16*, 43.



MoO<sub>2</sub> makes the nontopotactic route to Mo<sub>2</sub>C unavoidable. According to the results of XRD, Raman, and NMR, MoO<sub>3</sub> was first transformed mainly into MoO<sub>2</sub>, and increasingly *molybdenum oxycarbide* on the surface with increasing temperature, suggesting that the MoO<sub>3</sub> transformation to Mo<sub>2</sub>C is nontopotactic. We observed that MoO<sub>3</sub> is converted into MoO<sub>2</sub> at temperatures between 523 and 623 K, over which temperature range the carbon content remained very low, and this reduction is caused mainly by the hydrogen and not the butane. However, even for the sample produced at 623 K, an adequate <sup>13</sup>C NMR signal appeared, showing that there was carbon present. This process was further confirmed by the results of Raman measurements. As shown in Figures 3 and 4, the vibrations due to molybdenum oxide still exist (albeit weakly) in the samples carburized at temperatures up to 623 K. However, because the samples became black after carburization from 623 to 723 K, surface carbide formation must have been occurring. It is proposed that this surface carbide formation led to the virtual disappearance of the Raman spectra since the intensities of the bands became very weak. It should be noted, however, that the temperature was too low to effect the bulk of the sample as indicated by low values for carbon in the elemental analysis data, even though carbon was detectable by NMR, which shows that it existed in a fcc molybdenum lattice environment.

The TPre-MS results show that between 703 and 800 K water is produced and the butane flow decreases a little, suggesting that at this stage both hydrogen and butane are involved in the reduction process. By 823 K, according to the XRD data, the bulk of the sample has gained a fcc structure, even though some oxygen is still being evolved in the form of carbon oxides and water. Thus, by this temperature, the sample consists of fcc molybdenum carbide with a high oxygen concentration, i.e., the MoO<sub>x</sub>C<sub>y</sub> phase noted previously. However, it should be pointed out that the oxygen concentration rapidly diminishes with temperature and that most of the reduction i.e., oxygen loss, has already occurred, this being signaled by the high water profile in the MS data between 700 and 800 K. Having said this, some oxygen still persists in the sample, since water and carbon oxides continue to be evolved in the subsequent (higher temperature) reduction. This is also quite readily reconciled with reference to the TGA results, which do not show any well-defined features, but rather a general, featureless weight loss over this temperature range, consistent with there being a whole range of compositions possible. According to refs 36–38, molybdenum carbides can be formed at temperatures around 900 K using ethane as the carbon source. When using methane as a carbon source, carbide formation occurs close to 1000 K; hence, hexagonal Mo<sub>2</sub>C is formed directly under these conditions. Since carbide formation is observed by 750 K, these results suggest that butane is more active in the carburization of MoO<sub>3</sub> and that the intermediates formed during carburization are different from those for ethane and methane.

After carburization at 923 K, the structure of the reduced sample is still mainly fcc MoC<sub>1-x</sub>, but a considerable quantity of the hcp phase is also present, as indicated by XRD and carbon elemental analysis. Note-

worthy is the increased broadness of the XRD pattern for the hcp carbide, and also from the slight increase in BET surface area at 923 K, it appears that the particle size may be becoming smaller in association with the phase change. This is also supported by the NMR data which suggest that hcp Mo<sub>2</sub>C is present at these temperatures. After raising the carburization temperature to 1023 K, the sample consists mainly of the hexagonal Mo<sub>2</sub>C (XRD and NMR), but more importantly, no oxygenates are detected in the TPre-MS data, confirming that the oxygen in the carbide has been completely removed. Also, according to TPre-MS results, almost all of the butane was hydrogenated into methane after 900 K; thus, the final phase of the carburization process, from fcc MoC<sub>x</sub>O<sub>y</sub> to hexagonal Mo<sub>2</sub>C, was caused by methane. This reduction procedure provided both CO and CO<sub>2</sub> as products. Thus, this last stage in the reaction is the same as when methane is used as the carbon source.

**Chemical Reactions of Butane during the Carburization of MoO<sub>3</sub>.** Butane is not as thermally stable as methane and can undergo many reactions, some of which have been observed during the carburization process. According to the TPre-MS results, at temperatures below 793 K, the only reaction that appeared to be occurring was the reduction of MoO<sub>3</sub>; the butane shows little reactivity. However, above this temperature, carburization of the MoO<sub>2</sub>, to form the fcc carbide (strictly fcc molybdenum oxide–carbide solid solution), water and carbon oxides, started to occur along with other side reactions. These include the cracking of butane to give lower hydrocarbons such as methane, ethane, and possibly propane, but also formation of benzene. No xylenes or ethylbenzene was detected.

After the carburization temperature was raised to 910 K, a mixture of mainly fcc MoC and hcp Mo<sub>2</sub>C existed together with a low oxygen content. These phases together appear to be very active for methanation since from 910 to 1023 K, only methane existed in the gas phase. Efficient methanation is consistent with the noble metal character exhibited by molybdenum carbides; i.e., the highly reduced molybdenum sites found in the carbide display reactivity that resemble metals such as nickel. This type of reactivity is also in agreement with the observation that the phases have a very low oxygen concentration.

When the carburization temperature was raised above 1023 K, the catalyst consisted almost entirely of hexagonal Mo<sub>2</sub>C; however, it is also reasonable to assume that most of the bulk carbon deposition has occurred by these temperatures since the product distribution changes abruptly, implying that the active sites of the catalyst have been covered. At temperatures greater than 1023 K, only gas phase cracking occurs; it is suspected that the carbide plays little further role since the product distribution does not change with temperature. The products consist mainly of methane and C<sub>2</sub> products. Thus, from 703 to 1023 K, oxidation, cracking, and methanation reactions have all been observed, reflecting the ever decreasing oxygen concentration within the catalyst with increasing temperature.

**Catalytic Activity of the Carbide for Pyridine HDN and Dehydrogenation of Butane.** It has been shown that the electron-rich nature of molybdenum

carbide is similar to that of the noble metals, and it is active for reactions involving hydrogen activation.<sup>1,8,78</sup> In previous studies of pyridine HDN, the molybdenum carbide used has been prepared using methane as the carbon source: the activity and lifetime of these carbide catalysts were not satisfactory.<sup>73</sup> Our results show that the molybdenum carbide prepared using butane at 873 K can completely convert pyridine into nitrogen-free compounds initially, with a high selectivity to C4 and C5 alkane products. However, the activities of the catalysts MoC-823 K and MoC-1023 K were not as good. This may be due to the fact that MoC-873 K, which has fcc structure, still contains a moderate concentration of oxygen in the lattice or because the particle size is much smaller than for the carbide prepared using methane. The catalyst MoC-1023 K was not as active as MoC-873 K, probably because there is carbon deposited, which covers the active sites. The structure of MoC-1023 K is hexagonal Mo<sub>2</sub>C, which is the same as that prepared from methane at 1053 K. However, its activity is even lower than that of the carbide prepared from methane, further suggesting that a greater carbon deposit on MoC-1023 K is the main reason for the lower activity of the catalyst. The reason why MoC-823 K is less active is not clear, having both the lowest activity and the shortest lifetime. However, this may be tentatively attributed to insufficient carburization.

The nonoxidative dehydrogenation of lower alkanes into more valuable olefins or aromatics is a reaction that has received considerable attention.<sup>76,78–82</sup> It has been shown that ZSM-5 supported molybdenum oxide is a very effective catalyst for this reaction. Under the reaction conditions, the molybdenum oxide is converted into a carbide, which is probably the active phase, which when combined with the acidic nature of the ZSM-5 support works as a bifunctional catalyst, performing both dehydrogenation and isomerization. Gallo et al.<sup>57</sup> have pointed out that carbon-modified MoO<sub>3</sub> has a sufficiently acidic nature to catalyze the isomerization of butane. During carburization, it has been shown that dehydrogenation of butane to benzene could occur, even in the presence of a large excess of hydrogen. This indicates that the molybdenum carbides prepared with butane at temperatures between 793 and 900 K do display both noble metal and acidic characteristics. This is presumed to be due to the presence of both oxygen and carbon within the molybdenum lattice: careful control of the oxygen concentration is crucial. Hence, we carried out the dehydrogenation of butane over the molybdenum carbide material formed by the carburization of MoO<sub>3</sub> at 823 K for 2 h. This catalyst showed a conversion of butane of around 8% and a selectivity to benzene which was greater than 80%. The high selectivity to benzene is quite surprising, since we see no

conversion to xylenes or other C8-containing products. Further studies are continuing.

## Conclusions

Molybdenum carbide materials can be prepared using butane at a lower temperature than using either methane or ethane. In contrast to carbide preparation using either of these latter two gases, the fcc type structure of MoC<sub>x</sub>O<sub>y</sub> is formed at low temperatures using butane. Only after raising the carburization temperature above 1023 K does the MoC<sub>x</sub>O<sub>y</sub> change to hexagonal Mo<sub>2</sub>C. Transformation of MoO<sub>3</sub> to Mo<sub>2</sub>C during carburization with butane and hydrogen proceeds with a degree of topotacticity.

Solid-state NMR spectroscopy has been used to characterize the catalysts, and the data show two main types of carbon environment exist in the carbide materials. The broad resonance at 117 ppm in the <sup>13</sup>C NMR is assigned to carbon within fcc molybdenum lattice, while the peak at 273 ppm is assigned to molybdenum carbide with the hcp structure.

The reduction of MoO<sub>3</sub> with a mixture of H<sub>2</sub> and butane proceeds in several, albeit ill-defined, stages. The preliminary reduction of MoO<sub>3</sub> to MoO<sub>2</sub> is carried out with H<sub>2</sub>, during which period most of the high surface area was created. Subsequent reduction is mainly associated with butane. Once carburization begins, there is a gradual loss of oxygen from the lattice, which occurs more rapidly from the surface of the material and a phase change of molybdenum carbide material from monoclinic to face-centered cubic occurs. The cubic phase appears to allow an almost continuous range of oxygen and carbon solubility and may be called an oxycarbide phase. Higher temperature carburization leads to the β-Mo<sub>2</sub>C phase, which is the usual one produced from methane and ethane feedstocks. Above 1000 K carbon deposition occurs on the surface of the carbide along with sintering.

At higher carburization temperatures, butane is cracked and hydrogenated into methane, ethane, and propane. However, in the temperature range 800–900 K, dehydrogenation of butane over the oxycarbide phase also occurs, and the main product is benzene despite the high hydrogen concentration existing in the reactants.

Molybdenum carbide material prepared using butane at 873 K is a good catalyst for pyridine hydrodenitrogenation. The nitrogen from pyridine could be eliminated over this material at 653 K under a hydrogen atmosphere. The selectivity to C4 and C5 alkane products is very high. We have also shown that molybdenum carbide prepared from butane at temperatures between 773 and 823 K is active for the dehydrogenation, coupling, and isomerization of butane to benzene.

**Acknowledgment.** T. Xiao thanks the Royal Society for a Royal Society BP-AMOCO fellowship. We thank CANMET and the GRI for financial support for A. P. E. York, Pertamina for A. Hanif, King Abdulaziz City for Science and Technology for H. Al-Megren, and Colebrand Ltd. for support for V. C. Williams. We also thank J. B. Claridge for useful discussions.

CM001157T

(76) Lee, J. R.; Oyama, S. T.; Boudart, M. *J. Catal.* **1987**, *106*, 125.

(77) Benitez, V. M.; Querini, C. A.; Figoli, N. S.; Comelli, R. A. *Appl. Catal. A: Gen.* **1999**, *178*, 205.

(78) Zhang J.-Z.; Long, M. A.; Howe, R. F. *Catal. Today* **1998**, *44*, 293.

(79) Solymosi, F.; Szoke, A.; Cserenyi, J. *Catal. Lett.* **1996**, *39*, 157.

(80) Chen, L.; Lin, L.; Xu, Z.; Zhang, T.; Li, X. *Catal. Lett.* **1996**, *39*, 169.

(81) Wang, D. J.; Lunsford, J. H.; Rosynek, M. P. *J. Catal.* **1997**, *169*, 347.

(82) Liu, S.; Wang, L.; Ohnishi, R.; Ichikawa, M. *J. Catal.* **1999**, *181*, 175.